WATERHAMMER MODELING FOR THE ARES I UPPER STAGE REACTION CONTROL SYSTEM COLD FLOW DEVELOPMENT TEST ARTICLE

By

Jonathan Hunter Williams

A Thesis
Submitted to the Faculty of
Mississippi State University
in Partial Fulfillment of the Requirements
for the Degree of Master of Science
in Aerospace Engineering
in the Department of Aerospace Engineering

Mississippi State, Mississippi

December 2010

WATERHAMMER MODELING FOR THE ARES I UPPER STAGE REACTION CONTROL SYSTEM COLD FLOW DEVELOPMENT TEST ARTICLE

By

Jonathan Hunter Williams

Approved:

Masoud Rais-Rohani Professor of Aerospace Engineering (Graduate Advisor)	Gregory D. Olsen Engineer, AMRDEC (Committee Member)
David S. Thompson Associate Professor of Aerospace Engineering (Committee Member)	J. Mark Janus Associate Professor of Aerospace Engineering (Graduate Coordinator)
Sarah A. Rajala Dean of the James Worth Bagley College of Engineering	

Name: Jonathan Hunter Williams

Date of Degree: December 10, 2010

Institution: Mississippi State University

Major Field: Aerospace Engineering

Major Professor: Dr. Masoud Rais-Rohani

Title of Study: WATERHAMMER MODELING FOR THE ARES I UPPER STAGE REACTION CONTROL SYSTEM COLD FLOW DEVELOPMENT TEST ARTICLE

Pages in Study: 34

Candidate for Degree of Master of Science

The Upper Stage Reaction Control System provides three-axis attitude control for the Ares I launch vehicle during active Upper Stage flight. The system design must accommodate rapid thruster firing to maintain the proper launch trajectory and thus allow for the possibility to pulse multiple thrusters simultaneously. Rapid thruster valve closure creates an increase in static pressure, known as waterhammer, which propagates throughout the propellant system at pressures exceeding nominal design values. A series of development tests conducted in the fall of 2009 at Marshall Space Flight Center were performed using a water-flow test article to better understand fluid performance characteristics of the Upper Stage Reaction Control System. A subset of the tests examined waterhammer along with the subsequent pressure and frequency response in the flight-representative system and provided data to anchor numerical models. This thesis presents a comparison of waterhammer test results with numerical model and analytical results. An overview of the flight system, test article, modeling and analysis are also provided.

DEDICATION

To my wife. I am forever grateful for your patience and understanding through this long and drawn out process.

ACKNOWLEDGMENTS

This work was in support of NASA's Constellation Program and the Ares I Upper Stage Reaction Control System Development Test Article at Marshall Space Flight Center (MSFC). The opinions in this thesis belong solely to the author, and are not necessarily those of NASA.

First of all, I would like to thank Pat McRight and Chuck Pierce, my branch management here at NASA, for allowing me this opportunity to use my work at NASA as a foundation for my Master's thesis. I would like to thank Kim Holt for showing me the ropes in EASY5 and mentoring me over the past four years. Her knowledge of the software package and understanding of waterhammer were essential to my completion of this work over the past year. I would like to thank Ben Stein, Ph.D. for his help in troubleshooting and data analysis, as well as preparation of the conference paper that provided the foundation for this thesis [1]. With regards to the US ReCS SDTA testing, I would like to thank Melanie Dervan for her work as the US ReCS SDTA Lead. She provided excellent documentation and an overabundance of useful data for analysis purposes. Thanks also to John Wiley and his folks at the MSFC Component Development Area (CDA) for preparing the test article and running a great series of tests. Finally, I would also like to thank David Sharp and those at Jacobs Engineering for initially hiring me and allowing me to continue my education while working here at MSFC.

On the Mississippi State side, I would first off like to thank the entire Aerospace Engineering Department for a great and invaluable experience during my undergraduate and graduate degrees. Thanks to my committee for all of their valuable comments and insight during the preparation of this thesis. Thanks to Pasqualle Cinnella, Ph.D., Keith Koenig, Ph.D., and David Thompson, Ph.D. for teaching me the fundamentals of aerospace vehicles and fluids and laying the foundation for the work I do today. Thanks to Masoud Rais-Rohani, Ph.D. for picking me up and agreeing to be my graduate advisor during the final stages of this thesis work. And finally, thanks to Greg Olsen, Ph.D for allowing me the flexibility to switch research topics midstream and being supportive and understanding during the whole ordeal.

I would like to thank my parents for all their love and support over the last 27 years. Lastly, thanks to my wife for sticking with me through this and allowing me the time to finally put this behind me. Thanks for the final, and not-so-subtle, push to get this done.

TABLE OF CONTENTS

LIST OF TABLES

LIST OF FIGURES

LIST OF SYMBOLS, ABBREVIATIONS, AND NOMENCLATURE

ASME	American Society of Mechanical Engineers
CAD	Computer Aided Design
CDA	Marshall Space Flight Center Component Development Area
EASY5	MSC.EASY5 v.2008©
FFT	Fast Fourier Transform
FM	Turbine Flow Meter
Hz	Hertz
HfP	High-Frequency Pressure Transducer
lb_m	Pound mass
lb_f	Pound force
MDP	Maximum Design Pressure
MEOP	Maximum Expected Operating Pressure
msec	Milliseconds
MSFC	Marshall Space Flight Center
ND	Non-Dimensional
NV	Manual Metering Valve
PDR	Preliminary Design Review
PSD	Power Spectral Density

psi	Pounds per square inch
psia	Pounds per square inch, absolute
psig	Pounds per square inch, gauge
SDTA	System Development Test Article
sec	Seconds
TCV	Thruster Control Valve
TM	Thruster Module
US ReCS	Upper Stage Reaction Control System

CHAPTER 1

INTRODUCTION

1.1 Background

The development of the Ares I launch vehicle is an essential step toward completion of NASA's Constellation Program. This vehicle will facilitate a new generation of space access to the International Space Station, the moon, and other destinations within the solar system. Ares I is a two-stage launch vehicle consisting of a solid First Stage, a bipropellant Upper Stage, the Orion crew capsule and service module [2, 3]. The Upper Stage utilizes a single J-2X Main Engine fueled by a combination of liquid oxygen and liquid hydrogen. During Upper Stage operation, the Upper Stage Reaction Control System (US ReCS) will provide roll control capability during J2-X operation and three-axis attitude control capability (roll, pitch, and yaw) after Main Engine Cut-Off.

The US ReCS design utilizes a distributed, blow-down, monopropellant hydrazine system capable of rapid pulsing at the 100 lbf class. Past NASA launch vehicles such as the Saturn V [4] and the Space Transportation System (STS) [5] have employed localized, bipropellant systems for reaction control. The Delta IV [6] and Mars Polar Lander [7], developed by United Launch Alliance and Jet Propulsion Laboratory respectively, use attitude control systems similar to that of the US ReCS with the exception that they are pressure-regulated systems operated at lower thrust levels than the US ReCS. Therefore,

the combination of a distributed blow-down system with higher thrust levels makes the US ReCS, and all associated testing and analysis, relatively unique within the spacecraft propulsion community.

Additionally, the methods used at MSFC for transient fluid-flow analysis on the US ReCS vary from those documented in the literature for similar systems. Based on the literature review, the Method of Characteristics has proven to be the industry standard with regards to these analyses; however, the work done at MSFC for the US ReCS uses a Lumped Parameter Method. Past experience using both methods to model the same system has shown that both provide comparable results, with the exception being that the Lumped Parameter Method, with respect to its application in the modeling software, also allows for consideration of cavitation in the fluid which is not accounted for in the Method of Characteristics. In systems like the US ReCS, introduction of additional gas into the system through cavitation or other means can have a significant impact on the system dynamics and is thus important to characterize.

To date the analysis of these transient fluid-flows and their effects, specifically water-hammer, on spacecraft propulsion systems similar to the US ReCS have not been widely documented. Most available data for similar systems involve waterhammer due to priming the fluid system and not due to thruster valve closing. Additionally, data for waterhammer in response to thruster valve closing exists only for smaller and less complex systems [7, 8, 9, 10, 11, 12, 13]. Waterhammer is defined as a rise in static pressure inside a closed system resulting from a sudden deceleration of a fluid such as that caused by a valve closing. Viscous forces and tubing compliance tend to damp out the surge quickly,

with the peak pressure lasting only a few milliseconds. The resulting pressure surge due to valve closure can be more than twice the normal system operating pressure and can in itself cause significant damage to system tubing and hardware if not properly accounted for in the design. Additional concerns also arise if there is any residual gas remaining in the system. During the few milliseconds in which these events occur, a localized pressure increase can result in extreme heating of the gas due to a near-adiabatic compression. Given the right conditions, these high temperatures can result in an adiabatic compression detonation of the hydrazine at that location, which can lead to a catastrophic system failure. Due to these possible failure modes, requirements have been imposed upon the US ReCS design that the Maximum Design Pressure (MDP) of the system encompasses all transient surge pressure events. Therefore, it is important to sufficiently characterize US ReCS performance during different mission scenarios in order to provide a more robust design.

To accommadate this design process, development tests were conducted at MSFC in the fall of 2009 using a water-flow test article for the US ReCS in preparation for the Critical Design Review of the flight hardware. A variety of tests covering a range of supply pressures and duty cycles were conducted to examine system responses for different mission scenarios. Numerical models of the test article feed system were developed in conjunction with the development testing for post-test data correlation. The primary objective of these models was to accurately predict the initial surge pressure after valve closure, while secondary objectives included the prediction of other aspects of the system such as frequency and pressure response.

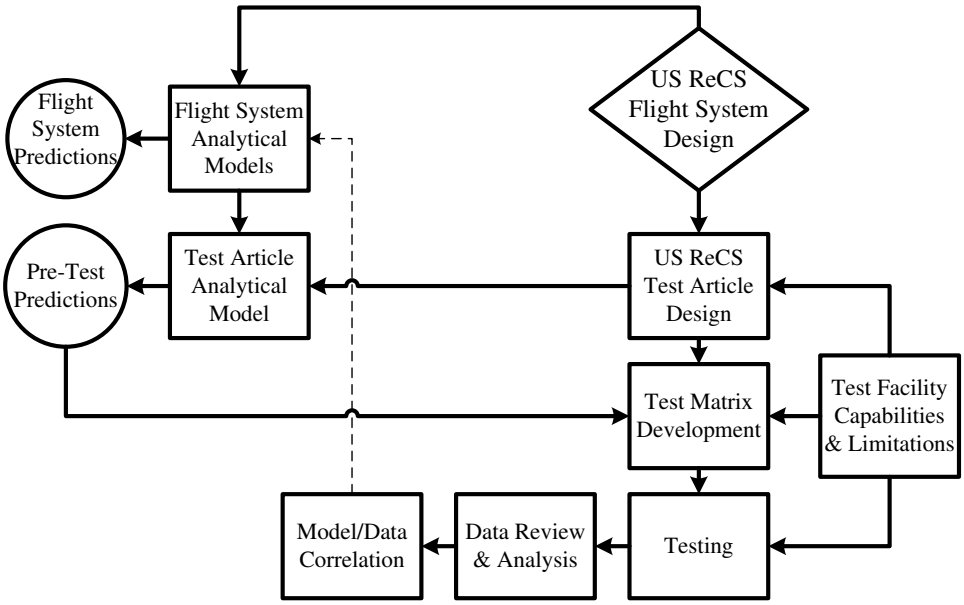

Figure 1.1

Flowchart for Design, Test, and Analysis Data and Information Flow

Figure 1.1 shows a general flowchart representation of the information and data flow through the system design, test, and analysis process. The chart shows how the flight system design provided input to both the numerical models and the development test article. The models of the flight system provided a foundation for the models of the test article. Pre-test predictions from these models along with the capabilities and limitations of both the test facility and test article were then used to develop the matrix of tests that were conducted. Tests were completed, and the resultant data was reviewed and analyzed. In addition, the data was used to correlate the numerical models of the test article such that they provided accurate predictions of the test article performance. From that point, the updates made to the models of the test article were flowed back up to the flight system models to provide a more accurate analytical representation of the flight system design.

1.2 System Description

1.2.1 Flight System

The US ReCS is a blow-down monopropellant system consisting of two diametrically opposed thruster modules (TM) mounted on the outer mold line of the Upper Stage Aft Skirt. Each TM in the US ReCS contains six 100-lbf class thrusters, three primary and three secondary, which in turn support the firing of multiple thrusters simultaneously for 3-axis attitude control. Hydrazine propellant is contained within a single diaphragm tank located on the J-2X thrust structure and is pressurized with gaseous helium. Performance requirements for a nominal blow-down specify a minimum 90 lbf vacuum thrust per thruster at the end of mission. The useable propellant load is 30 lbm. Based on these requirements, a diaphragm tank was designed for a 1.25:1 blow-down ratio with a maximum expected operating pressure (MEOP) of 420 psia. The pressurized tank expels the propellant through the main propellant feed line, which travels up the J-2X thrust structure to the Aft Skirt. It then branches to distribute propellant to each TM.

The US ReCS is also equipped with lines for propellant loading, draining, and decontamination. A single fill and drain line runs from the US ReCS service valve panel and connects to the propellant feed system downstream of the tank. Two system purge lines used for decontamination run from the service valve panel to each of the two TMs. A CAD (Computer Aided Design) representation of the system is shown in Figure 1.2, followed by a functional schematic in Figure 1.3.

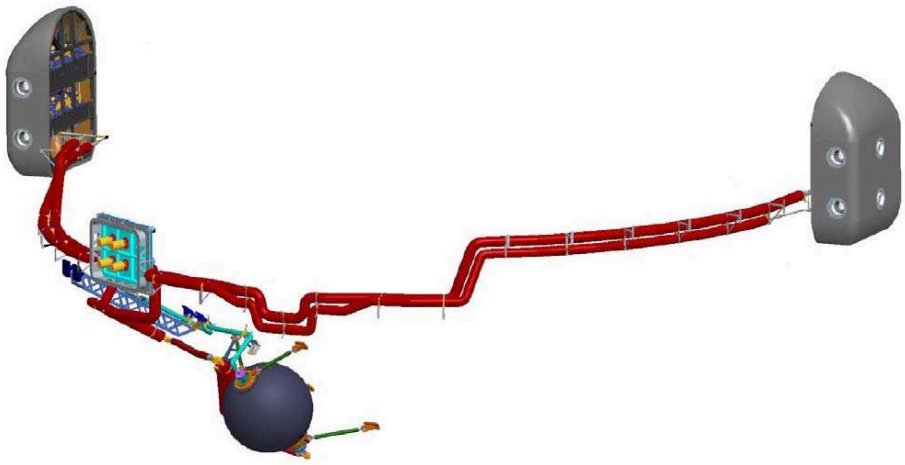

Figure 1.2

US ReCS CAD Representation

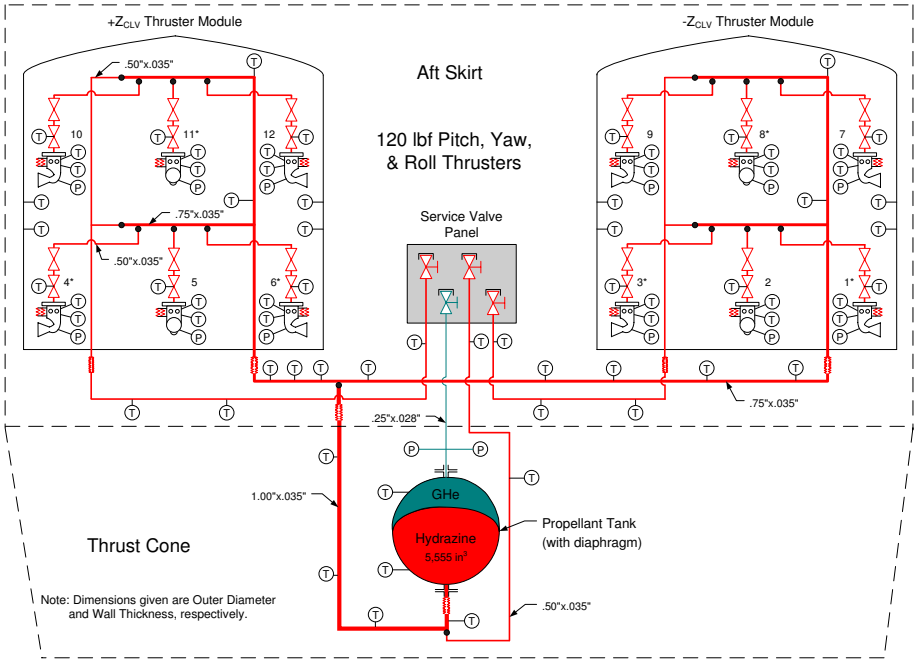

Figure 1.3

US ReCS Functional Schematic

1.2.2 System Development Test Article

1.2.2.1 Test Article Overview

The US ReCS System Development Test Article (SDTA) was a flight-representative simulator for the US ReCS flight system for Design Analysis Cycle 3A-S-RevA [14]. It was tested at the MSFC CDA to evaluate integrated system level performance characteristics and verify analytical models as part of the critical design activities. The SDTA used a single flight-similar diaphragm tank mounted in approximately the same relative location and orientation as the flight tank. An ASME (American Society of Mechanical Engineers) code tank was also incorporated into the test article for waterhammer testing to avoid excessive pressure cycling of the diaphragm tank and to test over a range of specified regulated pressures. A propellant distribution manifold representative of the flight configuration was fabricated with instrumentation ports for pressure transducers. Welded assemblies were used when possible to provide similarity to the flight propellant manifold, with exceptions at flex hose fitting connections, inlets to the Thruster Control Valve (TCV) assemblies, and break-point locations used to facilitate transportation. All SDTA components were mounted on a test fixture designed to decouple feed system dynamics, as shown in Figure 1.4. SDTA components were mounted to the test fixture using a similar approach to flight bracketing such that the dynamic response of the tubing was simulated.

Four TCV assemblies were fabricated for installation at four of the twelve possible locations within the thruster modules (L1 through L12 in Figure 1.5). These assemblies were capable of being moved between thruster valve locations depending on the required

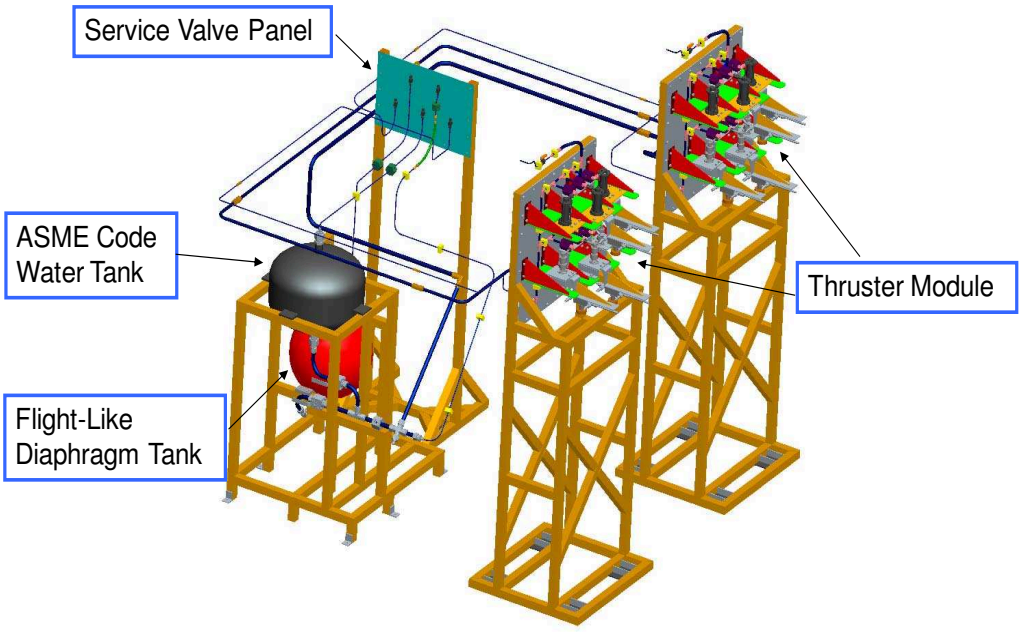

Figure 1.4

US ReCS SDTA CAD Representation

thrusters as specified for each test. The remaining locations were sealed to represent the total thruster module manifold. Each assembly included a series-redundant TCV, a manual metering valve, a turbine flow meter, and various instrumentation. The TCVs are denoted in Figure 1.5 by TCV-Xu (upstream) and TCV-Xd (downstream). Downstream of the TCVs, the manual metering valves (NV-X) allowed for flow rate calibration to a nominal flow rate similar to that of the flight system. Turbine flow meters (FM-X) were located downstream of the metering valves and measured the flow rate through the TCVs as controlled by the metering valves. Additional instrumentation on each assembly included thermocouples on the TCV and the downstream line, as well as a static pressure transducer upstream and downstream of the metering valve.

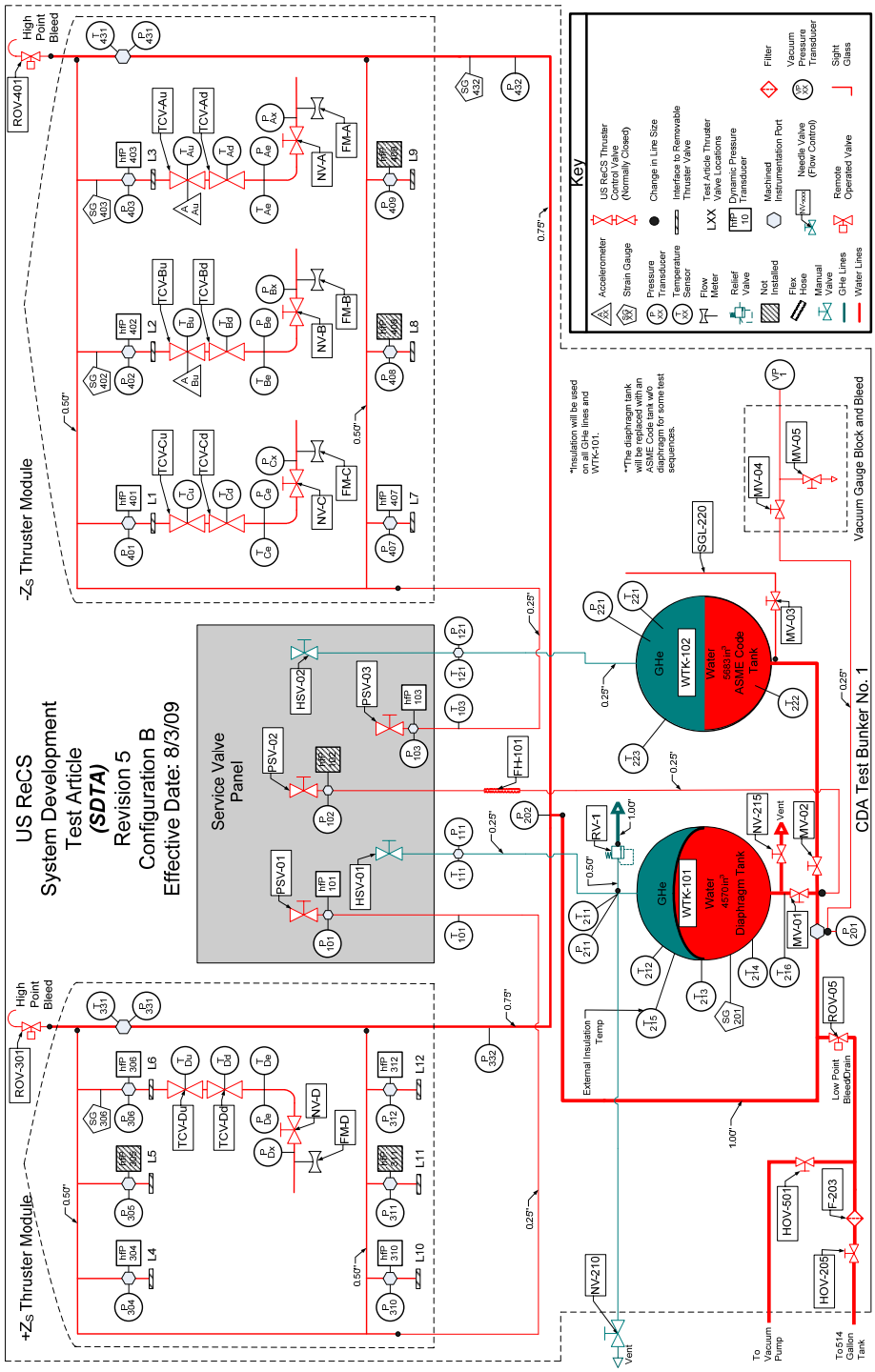

Figure 1.5

US ReCS SDTA Functional Schematic

1.2.2.2 System Instrumentation

Other system instrumentation included ten dynamic pressure transducers (HfP-XXX), one at the end of each purge line on the service valve panel and, due to data-system channel availability, one each at eight of the twelve TCV locations in the thruster modules. A breakdown of the system instrumentation by type is shown in Table 1.1 and is comparable to the instrumentation described in the literature for similar tests [10, 9, 7]. Dynamic pressure transducers and static pressure transducers were co-located in the same instrumentation block. Other static pressure measurements (P-XXX) were taken at various locations throughout the system and are shown in Figure 1.5. The pressurization system for both the diaphragm tank and the ASME code tank also contained multiple static pressure and temperature measurements. Other instrumentation included biaxial strain gauges at four of the twelve TCV locations to measure the effects of waterhammer on tubing, as well as accelerometers on TCVs A and B to provide data during valve actuation.

Table 1.1

System Instrumentation

Type	Quantity	Range	Data Rate (kHz)
Pressure Transducers - Static	33	0 to 2000 psig	10[1] 1[2]
Pressure Transducers - Dynamic	10	0 to 1000 to 5000 psid	50
Thermocouples	27	0 to 160°F	0.1
Accelerometers	2	0 to 25 g	50
Strain Guages	10	Axial and Hoop 0 - 70 μstrain	50
Flow Meters	4	FM-A: 2.0 - 12.4 GPM; FM-B, FM-C, FM-D: 0.6 - 5.0 GPM	1

1 For those adjacent to a dynamic transducer

2 Stand alone transducer

CHAPTER 2

MODELING AND ANALYSIS

2.1 Modeling in the Time Domain

Waterhammer can be modeled using many different methods, such as Finite Element Analysis [15], Method of Characteristics [7, 16, 17, 18, 19, 20, 21, 22, 23, 24, 25, 26], and Impedance Analysis [8, 22]. Another method for modeling waterhammer effects is the Lumped Parameter Method, which is employed by the EASY5 analysis package used at MSFC. MSCSoftware.EASY5 v.2008© is a commercially available, dynamic system modeling package with a heritage for modeling spacecraft propulsion systems. EASY5 is capable of modeling transient pressure wave phenomena, such as waterhammer, using transient forms of mass and energy conservation. The Thermal Hydraulic Library of EASY5 is a collection of fluid components (pipes, valves, orifices, etc.) whose input parameters and output variables are connected to other components to form complex fluid systems. EASY5 provides a robust modeling framework for waterhammer model development and was used to simulate various systems on Ares I. The EASY5 waterhammer model of the US ReCS SDTA, shown in Figure 2.1, was initially based on an existing US ReCS flight system model. However, throughout the SDTA data review and model correlation process, many updates and changes were made to reflect the differences between the

flight system and the test article. EASY5 components capable of modeling the transient pressure waves were used instead of steady-state alternatives.

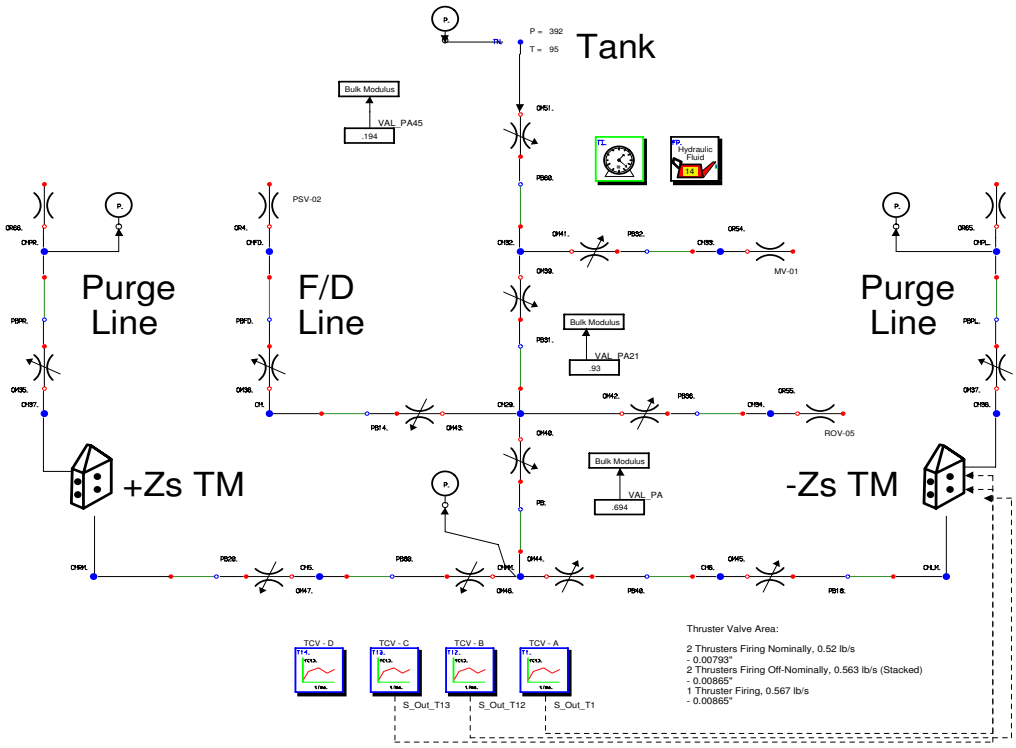

Figure 2.1

EASY5 Waterhammer Model US ReCS SDTA

2.1.1 Thruster Control Valve Assemblies

The model incorporated a transient-momentum orifice in the case of the TCV assemblies. It was sized for a nominal flow rate and could be commanded open and closed based on a pre-programmed duty-cycle. System characterization tests for the SDTA provided flow rate data for the TCV assemblies as a function of inlet pressure, as shown in Fig-

ure 2.2. The flow rate data for all TCV assemblies was combined and averaged, converted to a discharge coefficient as a function of inlet pressure, and then incorporated into the modeled TCV assemblies. Flow meter data measured downstream of the TCVs were also used to estimate a valve closing time. Likewise, high-frequency pressure data measured upstream of the TCVs were used to establish a closing profile for the valves, shown in Table 2.1, and represented the flow cross-sectional area as a function of time. Initially, this profile was assumed to be a linear closing over 0.5 msec, but upon inspection of the data a more parabolic closing profile over 0.4 msec was implemented in the model to better represent the data.

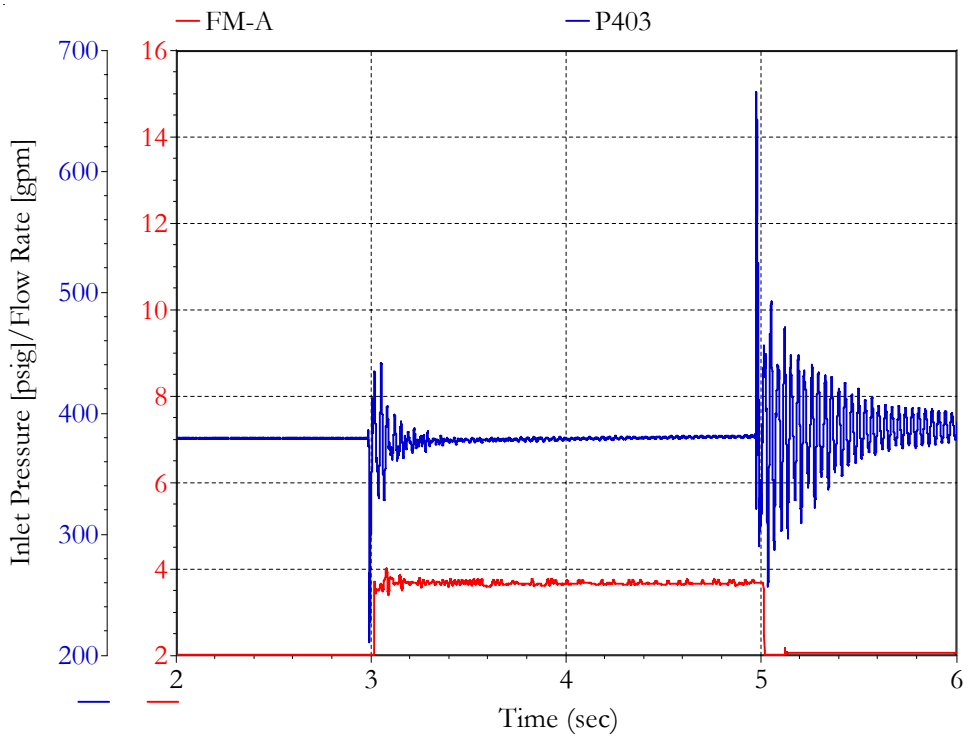

Figure 2.2

Typical Pressure and Flow Rate Response

Table 2.1

TCV Closing Profile

Time (msec)	Position *	Flow Area (in^2)
0	1	7.93×10^{-3}
0.3	0.75	5.95×10^{-3}
0.4	0	0.0

* (0=Closed, 1=Open)

2.1.2 System Tubing

Transient momentum pipe components were used for all the system tubing, from the tank outlet to the thruster valve inlets. The appropriate lengths and inner diameters were input into each component, along with the number of nodes for each pipe section. An increase in the number of nodes in each pipe section results in increased computational time for the model; therefore, an iterative process was used to determine the minimum number of nodes required to sufficiently characterize the waterhammer pressure wave for each pipe. The bulk modulus of the tubing material was input to produce more accurate speed of sound calculations within each pipe component. Pressure drops throughout the propellant feed system were initially based on analytical relations and flight system conditions but were updated to reflect the SDTA test data by modifying the surface roughness of each pipe component. A value for the tubing surface roughness was input based on published information for stainless steel tubing. An input in each pipe component for a frequency-dependent friction multiplier was also utilized to help dampen the pressure oscillations.

While relative height changes in tubing runs were included in the model, the contribution of tube bends to the pressure drop was considered negligible and was therefore not included in the model.

2.1.3 ASME Code Tank

The ASME code tank used for waterhammer testing was not specifically modeled in EASY5, but was represented as a boundary condition at a predefined pressure. This decision was justified based upon three reasons. First, the addition of the ASME code tank to the model would increase the complexity of the model and provide a significant negative impact on the run-time for each simulation. Second, only five milliseconds of steady-state flow were simulated prior to the valve closing, so the water-volume change in the tank was considered to be negligible. Third, with regards to the waterhammer event, neglecting to model the tank will ensure less overall system damping to the pressure wave and thus a more conservative result.

2.1.4 Entrained Gas

The capability to input the void fraction of entrained gas in a fluid also exists in EASY5 and affects the calculation of the fluid speed of sound and the system damping. The term void fraction refers to the ratio of the total volume of undissolved gas present at steady-state conditions to the total volume of the system, including both liquid and gas volume. This value is highly dependent on the initial conditions of the system prior to liquid filling and is one of the primary drivers behind vacuum-filling liquid propulsion systems similar

to the US ReCS. As more gas is introduced into the system, it decreases the bulk speed of sound of the fluid-gas mixture and increases the overall system damping. The void fraction of entrained gas was determined using the system geometry and the pre-water-load pad pressure. It was then possible to determine, assuming an isothermal compression, the final volume of displaced gas that would eventually be trapped by the liquid fill. The model assumed a homogenous mixture of gas and liquid, though realistically the bulk of the gas was trapped in various locations throughout the system. However, since it was impossible to determine with absolute certainty the location of those gas pockets, this assumption was the best that could be made.

2.2 Analysis in the Frequency Domain

Frequency analysis is a useful method for data analysis, especially with regard to determining the natural frequency and frequency matching in complex fluid systems such as the US ReCS SDTA. The Fast Fourier Transform (FFT) was employed to convert both experimental and simulation data into the frequency domain for analysis utilizing Power Spectral Density (PSD) curves [7]. MATLAB was used to perform FFTs to convert both experimental and simulation data into Power Spectral Density (PSD) curves to aid in data analysis and comparison. Straight-tube harmonics were also employed to provide a simple and quick way of estimating major system frequencies. Comparing these results to PSD curves of the test data and simulation results provided a secondary means for troubleshooting during the model correlation process in order to ensure that the major frequencies exhibited by the test article were captured by the fluid model.

2.3 Statistical Analysis

In addition to examining the data in both the time and frequency domain, statistical analyses were also employed to provide further comparisons between the test data and simulation results. Percent error for each individual pressure measurement were compared between tests, and average percent errors for entire tests were used as one of many metrics for establishing satisfactory agreement between the tests and simulations. Generally, the lower the average percent error the better with regards to these model correlations. Another tool utilized was standard deviations, which allowed the examination of the variation in measured pressure over multiple runs of a single test series. These values provided another means for troubleshooting during the model correlation process. Low standard deviations were indicative of consistent and repeatable pressure measurements, while high values suggested inconsistencies in the system between tests or possibly even instrumentation error.

CHAPTER 3

RESULTS AND DISCUSSION

3.1 Experimental

Eighty-two tests specific to waterhammer were conducted during testing of the US ReCS SDTA using an array of supply pressures, TCV sequences, TCV configurations, and overall system configurations. Most TCV sequences were run at a low (315 psia), nominal (385 psia), or high supply pressure (410 psia) in reference to the flight system MEOP of 420 psia. Testing was performed in three different system configurations. The first configuration is represented schematically in Figure 1.5. TCVs A, B and C were located at L3, L2, and L1, respectively, in the -Z_s Thruster Module (TM) with TCV-D being located at L6 in the +Z_s TM. The second configuration required repositioning of two TCVs such that each TM was configured with a primary and redundant roll TCV. TCVs A and B were relocated to L7 and L12 respectively, while TCVs C and D remained in the same locations (L1 and L6, respectively). The third configuration was the same as the second configuration with the exception that the purge lines were removed. The surge pressures measured at the service valves in the purge lines met or exceeded those measured in the TMs during many of the previous tests; therefore, a third configuration was tested.

Out of the eighty-two total waterhammer tests, a set of twelve nominal baseline tests were conducted using the first configuration to provide data points to demonstrate system

repeatability during testing. One of the twelve tests (test WH6r) was chosen as a baseline for model correlation due to the simplistic nature of the test. Test WH6r used a supply pressure of 395 psia and a duty cycle of eight two-second pulses, as shown in Table 3.1 [27]. A typical pressure response measured at HfP-403 at the inlet of TCV-A for a single pulse during test WH6r is shown in Figure 3.1.

Table 3.1

Duty Cycle WH6, used for Test WH6r

Time (sec)	TCV-A	TCV-B	TCV-C	TCV-D
0.0	OPEN	CLOSED	CLOSED	CLOSED
2.0	CLOSED	-	-	-
4.0	-	OPEN	-	-
6.0	-	CLOSED	-	-
8.0	-	-	OPEN	-
10.0	-	-	CLOSED	-
12.0	-	-	-	OPEN
14.0	-	-	-	CLOSED
16.0	OPEN	-	-	-
18.0	CLOSED	-	-	-
20.0	-	OPEN	-	-
22.0	-	CLOSED	-	-
24.0	-	-	OPEN	-
26.0	-	-	CLOSED	-
28.0	-	-	-	OPEN
30.0	-	-	-	CLOSED

The data displayed in Figure 3.1 show the closure of TCV-A in test WH6r at 4.97 seconds, as measured by HfP-403. The resultant pressure oscillations resemble a decaying sinusoid, a behavior typical of fluid damping and frictional effects. The amplitude of the pressure wave decayed exponentially and resulted in pressure reductions of 25% within

50 msec and 95% within 500 msec. The wave continued to dampen, approaching the static supply pressure before the next pulse was initiated. The peak pressure for this case was approximately 830 psia using HfP-403 at the inlet of TCV-A, with a slightly lower pressure of 785 psia measured in the corresponding purge line at HfP-103.

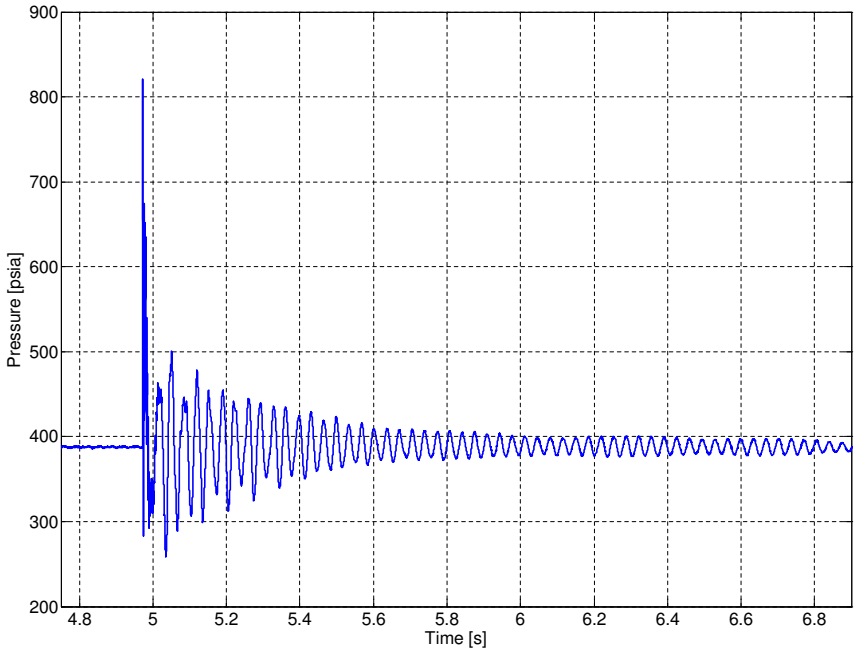

Figure 3.1

Pressure Response During Test WH6r at TCV-A

Figure 3.2 represents the frequency response of the system at HfP-403 for test WH6r, with the natural frequency of the system occurring at approximately 30 Hz. It was found that the resulting PSD curve for the static pressure transducer data exhibited a structure similar to that of the high frequency transducer data. Pressure data at all TCVs were compared and produced results similar to Figure 3.2, both in magnitude and frequency.

This suggests the frequency spectrum of the pressure data within the TMs are equivalent, irrespective of pressure transducer location. The pressure data at the TCV locations were then compared to that recorded at the purge valves. The PSD curve at each purge valve also produced a similar spectrum to that present in the TMs.

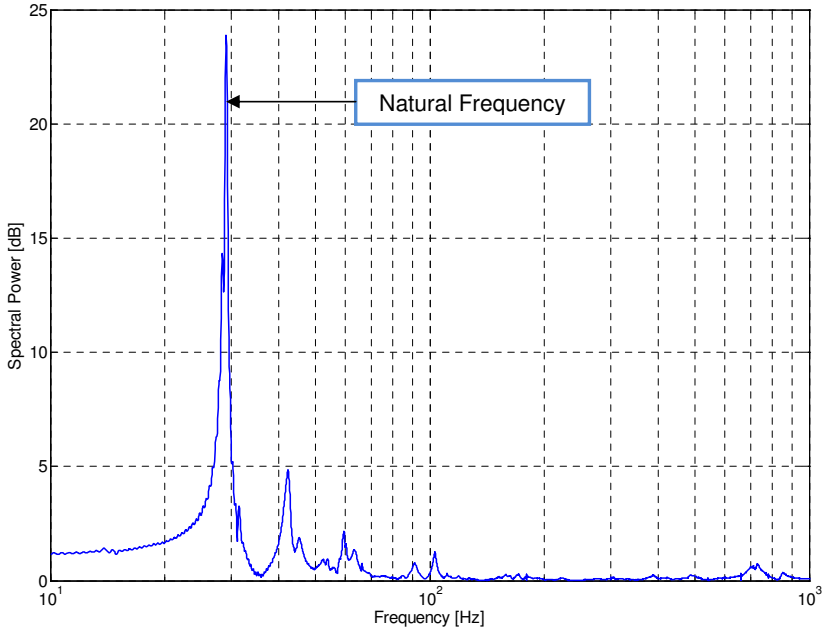

Figure 3.2

Frequency Domain Representation of Experimental SDTA Data

3.2 Analytical vs. Experimental

Simulations for the US ReCS SDTA EASY5 model were run using the methodology laid out in the previous chapter. The appropriate values for system dimensions were input, along with friction parameters and a gas-liquid void fraction. Pre-test predictions showed good correlations for maximum surge pressure to within 15% of the test data. The flow

rates and pressure drops through the system also matched well with the test data. However, other aspects of the model results, such as the damping and frequency of the pressure response, exhibited significant differences. The simulation results were underdamped and displayed a higher natural frequency (approximately 45 Hz) than that of test data, though the natural frequency did change slightly from test to test. This change in frequency between tests could be attributed to varying amounts of water in the ASME code tank, as well as the amount and location of trapped gas in the system.

Modifications were made to the model in several areas in an attempt to correct these discrepancies. The number of nodes in each pipe segment was examined and, in most cases, increased in order to refine each segments ability to capture the amplitude of the pressure wave. A range of values for both the frequency dependent friction multiplier and the gas-liquid void fraction were examined to determine their effects on both frequency and damping. FFTs of both the test data and simulation results were also employed in an attempt to identify the source of the frequency differences. The high-frequency pressure measurement (HfP-403) at the inlet of TCV-A for the first pulse of test WH6r was used during these modifications for model calibration.

The final simulation and analysis results compared with test WH6r are shown for the time domain in Figures 3.3 and 3.4 and for the frequency domain in Figure 3.5. Since the calculations for MDP only include the maximum surge pressure seen in the system, regardless of where it occurs, Table 3.2 shows the comparison of the maximum pressures in the test data versus that from the simulations. The maximum surge pressure in the system was predicted to within 2.5% (Table 3.2), an approximate 12.5% improvement over the

pre-test predictions. It should be noted that the EASY5 model predicts the maximum surge pressure to occur at HfP-103 in the -Z_s TM purge line, whereas the test data shows the maximum occurring at HfP-403 in the -Z_s TM at the inlet to TCV-A. For HfP-403, the model predicts the surge pressure to within 2.0%.The average percentage error for all high frequency pressure measurements throughout the system for the initial surge pressure peak was 5.21%.

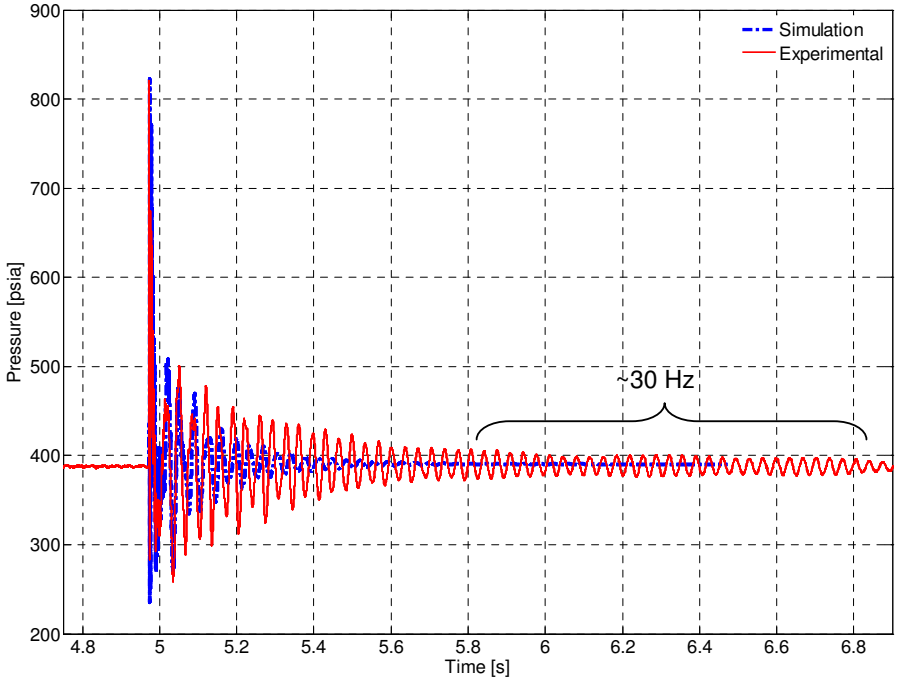

Figure 3.3

Test vs. Simulation: Full Simulation

The model also predicts the natural frequency of the system around 30 Hz, along with other notable frequencies found in the test data at approximately 40 Hz and in the 700-800 Hz range. The 40 Hz frequency is thought to correspond to the propagation of pressure

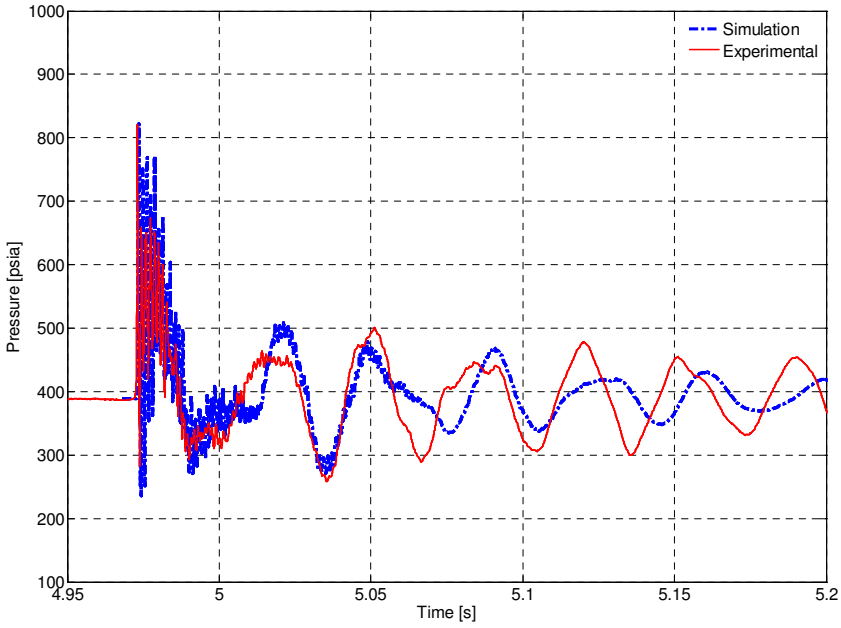

Figure 3.4

Test vs. Simulation: TCV closure and the first few pressure oscillations

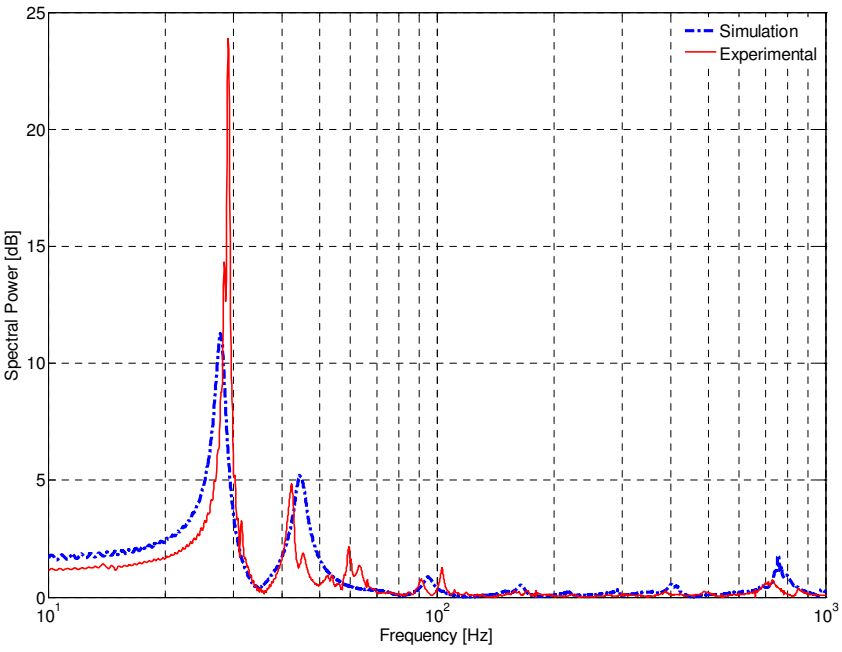

Figure 3.5

Test vs. Simulation: PSD Curves for HfP-403 at TCV-A

Table 3.2

Percent Error Between Test Data and Model Predictions

Pressure Measurement*	WH4b			WH4c			WH4r		
	Test	Model	% Error	Test	Model	% Error	Test	Model	% Error
HfP-101	540	528	2.22%	531	528	0.56%	518	525	1.35%
HfP-103	623	683	9.63%	621	683	9.98%	622	679	9.16%
HfP-304	429	435	1.40%	428	435	1.64%	419	433	3.34%
HfP-306	439	427	2.73%	434	427	1.61%	423	425	0.47%
HfP-310	345	427	23.77%	361	427	18.28%	416	424	1.92%
HfP-312	362	427	17.96%	382	427	11.78%	411	424	3.16%
HfP-401	571	506	11.38%	553	506	8.50%	542	503	7.20%
HfP-402	542	529	2.40%	540	529	2.04%	560	526	6.07%
HfP-403	676	678	0.30%	640	678	5.94%	687	674	1.89%
HfP-407	520	567	9.04%	500	567	13.40%	477	564	18.24%
Maximum Pressure	676	683	**1.04%**	640	683	**6.72%**	687	679	**1.16%**
Average Percent Error			***8.08%***			***7.37%***			***5.28%***
Pressure Measurement*	**WH5b**			**WH5c**			**WH5r**		
	Test	**Model**	**% Error**	**Test**	**Model**	**% Error**	**Test**	**Model**	**% Error**
HfP-101	640	638	0.31%	646	643	0.46%	632	627	0.79%
HfP-103	746	766	2.68%	744	773	3.90%	757	802	5.94%
HfP-304	515	529	2.72%	519	534	2.89%	509	521	2.36%
HfP-306	521	525	0.77%	528	530	0.38%	517	512	0.97%
HfP-310	420	526	25.24%	446	531	19.06%	506	511	0.99%
HfP-312	437	522	19.45%	469	527	12.37%	503	512	1.79%
HfP-401	662	636	3.93%	692	642	7.23%	675	601	10.96%
HfP-402	637	627	1.57%	660	633	4.09%	656	629	4.12%
HfP-403	776	801	3.22%	827	808	2.30%	813	798	1.85%
HfP-407	614	644	4.89%	628	650	3.50%	607	672	10.71%
Maximum Pressure	776	801	**3.22%**	827	808	**2.30%**	813	802	**1.35%**
Average Percent Error			***6.48%***			***5.62%***			***4.05%***
Pressure Measurement*	**WH6b**			**WH6c**			**WH6r**		
	Test	**Model**	**% Error**	**Test**	**Model**	**% Error**	**Test**	**Model**	**% Error**
HfP-101	675	663	1.78%	671	661	1.49%	658	666	1.22%
HfP-103	828	847	2.29%	784	843	7.53%	784	850	8.42%
HfP-304	547	553	1.10%	540	550	1.85%	533	555	4.13%
HfP-306	552	543	1.63%	548	541	1.28%	540	546	1.11%
HfP-310	448	543	21.21%	465	540	16.13%	524	545	4.01%
HfP-312	466	543	16.52%	489	541	10.63%	521	546	4.80%
HfP-401	719	637	11.40%	721	634	12.07%	727	640	11.97%
HfP-402	700	666	4.86%	684	663	3.07%	688	669	2.76%
HfP-403	834	842	0.96%	857	839	2.10%	831	846	1.81%
HfP-407	655	710	8.40%	655	707	7.94%	637	713	11.93%
Maximum Pressure	834	847	**1.56%**	857	843	**1.63%**	831	850	**2.29%**
Average Percent Error			***7.01%***			***6.41%***			***5.21%***

waves between the thruster modules and the tank, while the 700-800 Hz frequencies are thought to be oscillations within the thruster modules themselves. These notions are based on calculations performed using simple straight tube harmonics; therefore, a more in-depth analysis will be required to confirm the source of these frequencies. Comparisons were also made with eight other tests that employed the same duty cycle as test WH6r. With exception for the supply pressure, inputs for the EASY5 waterhammer model remained constant for all eight test cases to provide consistency between the simulations. The approximate supply pressure was 310 psia for the tests designated with WH4*x*, 380 psia for WH5*x*, and 400 psia for WH6*x*. The results of these comparisons are tabulated along with the baseline case, WH6r, in Table 3.2. The results for all nine tests showed the maximum surge pressures predicted to within 6.72 %, with the average percent error for all pressure measurements to within 8.08%.

3.3 Resolution of Discrepancies and Error

A primary difference between the simulation and experimental data is that the simulation damps out faster than the experimental data (Figure 3.3), resulting in an underprediction of the amplitude of the natural frequency (Figure 3.5) [28]. This result was consistent across all the simulations that were run and compared with test data. It is believed this discrepancy in the magnitude of the natural frequency (i.e. system damping) is due to one or more characteristics of the US ReCS SDTA (e.g. ASME code tank, fluid/structure interaction, frequency-dependent friction, etc.) that are currently unaccounted for or modeled incorrectly in the EASY5 model. Since accurate prediction of the system damping was not

the primary objective of the system modeling and proved to have little to no impact on the peak surge pressure, the discrepancy was accepted and deferred as future work. Updating the EASY5 waterhammer model for both the test article and the flight system will focus on establishing a better correlation between the model and test data with regards to damping in hopes to get rid of this disparity.

Another error, which can be noted from Table 3.2, is that two of the ten measurements (HfP-310 and HfP-312) consistently exhibit higher error (greater than 10%) than the other eight. The most likely explanation for these errors is high variability in those individual pressure measurements from test to test. Figures 3.6, 3.7, and 3.8 provide a comparison of the percent error in the predicted pressure measurements versus the standard deviation of each pressure measurement. Each figure contains plots of the percent error in predicted measurements for three separate runs of a single test series (i.e. WH4b, WH4c, WH4r), as well as a plot of the standard deviation of each pressure measurement across those three runs. In order to account for different static inlet pressures for the different tests compared, the pressure measurements (i.e. the peak surge pressure values) were non-dimensionalized with respect to their reference static inlet pressures.

The results shown in Figures 3.6, 3.7, and 3.8 illustrate a strong correlation between high percent error and high variability in the pressure measurements. The pressure measurements HfP-310 and HfP-312 consistently showed the highest error across all the tests examined, and consistently those measurements also had the highest variability from test to test. High variability in the pressure measurement could be caused by a number of things. Based on the results shown in Table 3.2, the model over-predicted the pressures at

those two locations, which corresponded to locations in the system that never experienced flow. It is likely that during the initial water fill process, residual gas in the system became trapped at these locations and damped the pressure response measured by the transducer at those locations. Regardless of the reason for the error, these areas of high variability ultimately result in parts of the system that are less predictable and more difficult to model. There is no way to predict from test to test where these areas of high variability will occur, other than they seem to tend more toward the areas of low or no flow based on the data that has been examined thus far. For future analyses and simulations, it will have to be decided on a case by case basis how these are handled to most accurately reflect the system being modeled.

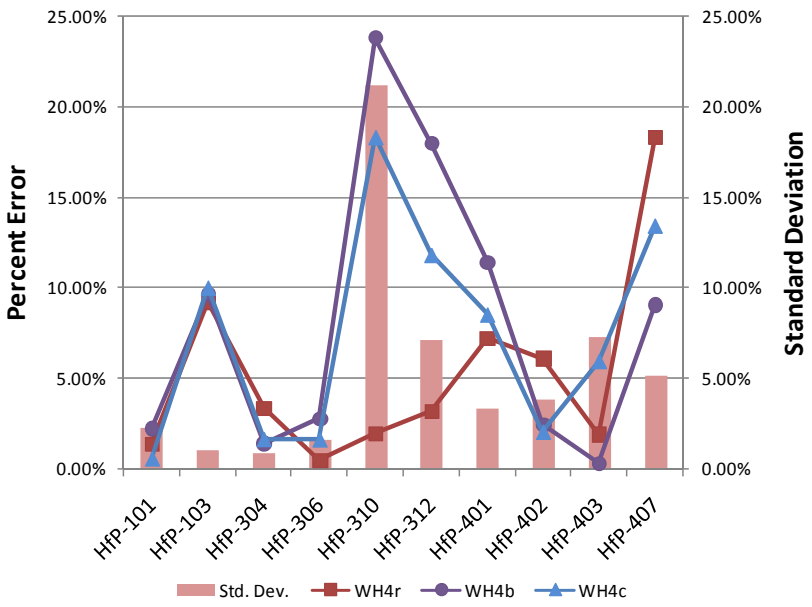

Figure 3.6

Percent Error vs. Standard Deviation for Duty Cycle WH4

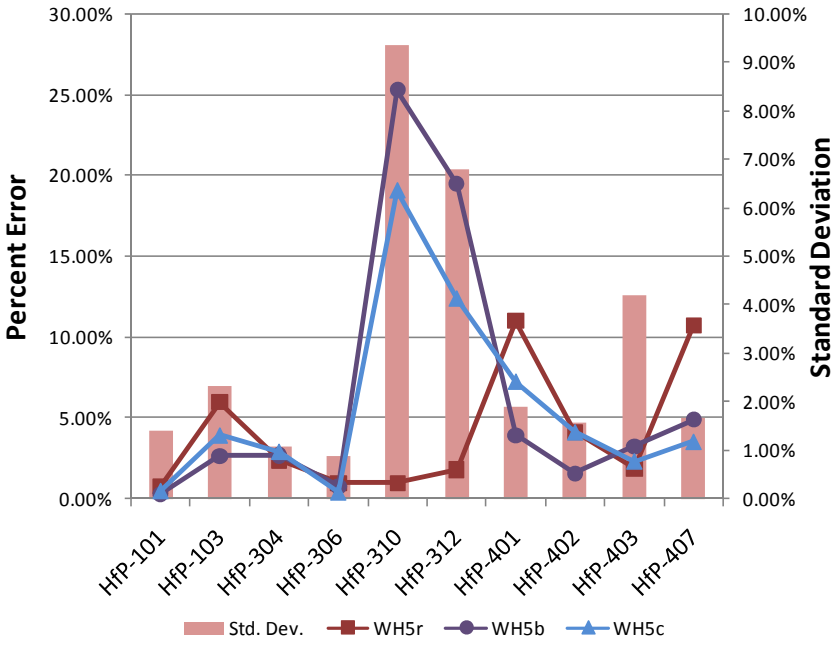

Figure 3.7

Percent Error vs. Standard Deviation for Duty Cycle WH5

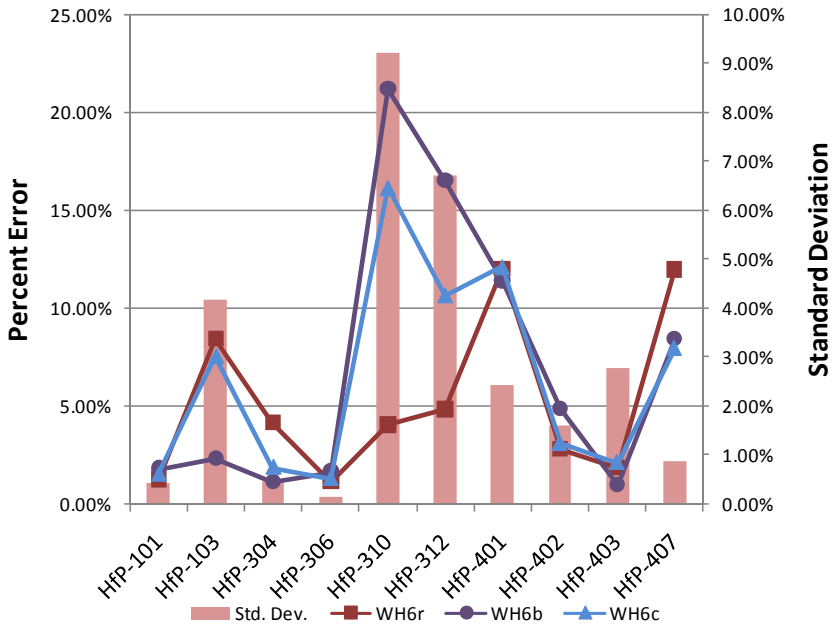

Figure 3.8

Percent Error vs. Standard Deviation for Duty Cycle WH6

CHAPTER 4

CONCLUSIONS

Waterhammer tests were performed using the US ReCS SDTA to provide anchoring data for numerical models of the US ReCS flight system. Comparisons of the simulation results to multiple sets of test data for the SDTA showed strong correlations for both the pressure and frequency responses of the system. Maximum surge pressures from the test data were predicted to within 6.75% by the EASY5 model. The natural frequency of the system was not captured as strongly in the model as it was in the test data as a result of the overdamping of the waterhammer pressure wave in the simulations. Future work will focus on improvements to the EASY5 model to provide better correlation with the system damping. In addition, tests involving multiple TCV closings will be examined and compared to simulation results. The results presented within this thesis validate the models ability to predict system performance of the SDTA and provide confidence that the maximum surge pressures can be accurately modeled and predicted for the US ReCS flight system.

REFERENCES

[1] J. Williams, K. Holt, and W. Stein, "Testing and Modeling of the Ares I Upper Stage Reaction Control System," *Proceedings: 57th JANNAF Propulsion Meeting*, Colorado Springs, CO, 2010, JANNAF, JANNAF-1163.

[2] M. Dervan, J. Williams, K. Holt, J. Wiley, A. Sivak, and J. Morris, "NASA Ares I Upper Stage Reaction Control System Cold Flow Development Test Program Results," *Proceedings: 57th JANNAF Propulsion Meeting*, Colorado Springs, CO, 2010, JANNAF, JANNAF-1370.

[3] A. Turpin, *Upper Stage Reaction Control System (ReCS) Subsystem Design Specification*, Tech. Rep., National Aeronautics and Space Administration, Ares-USO-SE-25718.

[4] *Saturn Technical Information Handbook*, Tech. Rep., George C. Marshall Space Flight Center, May 1966, NASA-TM-109688.

[5] *Space Shuttle Orbiter Reaction Control Subsystem Smartbook*, Tech. Rep., Rockwell International, November 1989, Ares-USO-SE-25718.

[6] D. M. Hart, "The Boeing Company EELV/Delta IV Family," *Proceedings: Defense and Civil Space Programs Conference*. AIAA, 1998, AIAA-1998-5166.

[7] T. Martin, L. Rockwell, and C. Parish, "Test and Modeling of the Mars 98 Lander Descent Propulsion System Waterhammer," AIAA, 1998, AIAA-98-3665-858.

[8] A. Malesiska, M. Chorzelski, and M. Mitosek, "Experimental analysis of natural frequency of water column due to water hammer in series pipe systems," Warsaw, 2002, ICHSE.

[9] W. H. Hsieh, C. Y. Lin, and A. S. Yang, "Blowdown and Waterhammer Behavior of Mono-propellant Feed Systems for Satellite Attitude and Reaction Control," AIAA, 1997, AIAA-1997-3224-161.

[10] I. Gibek and Y. Maisonneuve, "Waterhammer Tests with Real Propellants," *Proceedings: 41st Joint Propulsion Conference*. AIAA, 2005, AIAA-2005-4081.

[11] R. Lecourt and J. Steelant, "Experimental Investigation of Waterhammer in Simplified Basic Pipes of Satellite Propulsion Systems," *Journal of Propulsion and Power*, vol. 23, no. 6, November-December 2007, pp. 1214–1224.

[12] R. P. Prickett, E. Mayer, and J. Hermel, "Water Hammer in a Spacecraft Propellant Feed System," *Journal of Propulsion and Power*, vol. 8, no. 3, May-June 1992, pp. 592–597.

[13] J. Molinsky, "Water Hammer Test of the SeaStar Hydrazine Propulsion System," *Proceedings: 33rd Joint Propulsion Conference*. AIAA, 1997, AIAA-97-3226.

[14] M. Dervan, *US ReCS System Level Cold Flow Development Test Plan*, Tech. Rep., National Aeronautics and Space Administration, RCS-PLAN-DTP-030.

[15] R. Leishar, "Dynamic Pipe Stresses During Waterhammer: A Finite Element Approach," *ASME Journal of Pressure Vessel Technology*, vol. 129, May 2007.

[16] E. Wylie, *Resonance in Pressurized Piping Systems*, doctoral dissertation, The University of Michigan, November 1964.

[17] W. Zielke, *Frequency Dependent Friction in Transient Pipe Flow*, doctoral dissertation, The University of Michigan, December 1966.

[18] E. Wylie and W. Zielke, *Propellant Line Dynamics*, Final report, The University of Michigan, September 1967.

[19] D. M. Contractor, *The Effect of Minor Losses on Waterhammer Pressure Waves*, doctoral dissertation, The University of Michigan, December 1963.

[20] C. Lai, *A Study of Waterhammer Including Effect of Hydraulic Losses*, doctoral dissertation, The University of Michigan, December 1961.

[21] W. Yow, *Analysis and Control of Transient Flow in Natural Gas Piping Systems*, doctoral dissertation, The University of Michigan, 1971.

[22] V. L. Streeter, *Computer Solutions of Surge Problems*, Report, The University of Michigan, Februaryr 1965, IP-694.

[23] V. L. Streeter, *Waterhammer Analysis with Nonlinear Frictional Resistance*, Report, The University of Michigan, August 1962, IP-579.

[24] V. L. Streeter, *Waterhammer Analysis of Pipelines*, Report, The University of Michigan, November 1963, IP-642.

[25] V. L. Streeter, *Valve Stroking for Complex Piping Systems*, Report, The University of Michigan, October 1966, IP-747.

[26] V. L. Streeter, *Waterhammer Analysis of Distribution Systems*, Report, The University of Michigan, October 1966, IP-748.

[27] J. H. Williams, "US ReCS SDTA Test Matrix," Version 10, July 2009.

[28] L. Ounougha and F. Colozzi, *Correlation Between Simulations and Experiments on Water Hammer Effects in Propulsion System,* Final report, European Space Agency, August 1997.